Original Article

Specific effects of hypoxia-immune core gene *ARHGAP11A* on lung adenocarcinoma

Kang Sun[1,2], Luyao Wang[3], Xueying Zhang[1], Huili Chen[2], Ziqiang Wang[2], Jing Zhang[3], Xiaojing Wang[1], Chaoqun Lian[2]

[1]Anhui Province Key Laboratory of Respiratory Tumor and Infectious Disease, Department of Pulmonary and Critical Care Medicine, Molecular Diagnosis Center, First Affiliated Hospital of Bengbu Medical University, Bengbu, China; [2]Research Center of Clinical Laboratory Science, Bengbu Medical University, Bengbu, China; [3]Department of Genetics, School of Life Sciences, Bengbu Medical University, Bengbu, China

Contributions: (I) Conception and design: K Sun, C Lian, X Wang, J Zhang; (II) Administrative support: C Lian, X Wang, J Zhang; (III) Provision of study materials or patients: K Sun, X Zhang, L Wang; (IV) Collection and assembly of data: K Sun, L Wang, X Zhang; (V) Data analysis and interpretation: K Sun, H Chen, Z Wang; (VI) Manuscript writing: All authors; (VII) Final approval of manuscript: All authors.

Correspondence to: Xiaojing Wang, PhD. Anhui Province Key Laboratory of Respiratory Tumor and Infectious Disease, Department of Pulmonary and Critical Care Medicine, Molecular Diagnosis Center, First Affiliated Hospital of Bengbu Medical University, 287 Changhuai Avenue, Bengbu 233000, China. Email: wangxiaojing8888@163.com; Chaoqun Lian, PhD. Research Center of Clinical Laboratory Science, Bengbu Medical University, 2600 Donghai Avenue, Bengbu 233000, China. Email: lianchaoqun@bbmc.edu.cn.

Background: The changes in tumor microenvironment (TME) are closely related to the regulation of immunity and hypoxia. This study aimed to investigate the specific effects of *ARHGAP11A* on the prognosis, immunity, and hypoxia of lung adenocarcinoma (LUAD).

Methods: The core gene *ARHGAP11A* related to immunity and hypoxia was obtained from a variety of databases, including Gene Expression Omnibus (GEO), The Cancer Genome Atlas (TCGA), Human Protein Atlas (HPA), Tumor Immune Estimation Resource (TIMER), the Search Tool for the Retrieval of Interacting Genes (STRING), HALLMARK gene set, and various analysis methods (differences and single factor Cox analysis). The relationship between the expression level of *ARHGAP11A*, survival prognosis, immune invasion, and hypoxia regulation was analyzed.

Results: *ARHGAP11A* was associated with poor patient prognosis and was strongly associated with immune and hypoxic-related signal pathways. We also found that knocking down the expression of *ARHGAP11A* can affect the proliferation, glycolysis, migration, invasion, and anti-apoptotic ability of tumor cells. The changes of apoptosis-related proteins (BCL2, BAX, and Caspase-3), cell cycle protein E1, D1 (cyclin D1, cyclin E1), matrix metalloproteinase 2 and 9 (MMP2, MMP9), and P-Phosphatidylinositol 3-kinase and protein kinase B (P-PI3K and P-AKT) in the knockdown group, were verified by Western blot (WB). We also found that interfering with the expression of *ARHGAP11A* can reduce the expression of programmed cell death ligand 1 (PDL1) in LUAD cells. Through the induction of tumor cells by cobalt chloride (CoCL2), we established a hypoxic microenvironment, and found that interfering with *ARHGAP11A* can significantly reduce the expression of hypoxia-inducible factor 1A (*HIF1A*), downstream molecular vascular endothelial growth factor A (VEGFA), and lactate dehydrogenase A (LDHA).

Conclusions: The expression of *ARHGAP11A* is highly correlated with immunity, hypoxia, poor prognosis, and tumor cell development. Therefore, the study of *ARHGAP11A* can provide more ideas on comprehensive treatment and prognosis management of LUAD.

Keywords: Lung adenocarcinoma (LUAD); *ARHGAP11A*; immune microenvironment; hypoxia; prognosis

Submitted Feb 05, 2024. Accepted for publication Dec 06, 2024. Published online Feb 26, 2025.
doi: 10.21037/tcr-24-224
View this article at: https://dx.doi.org/10.21037/tcr-24-224

Introduction

Lung cancer is the most frequently observed cause of cancer death in the USA, with non-small cell lung cancer (NSCLC) being the most common type, of which the most important subtype of NSCLC is lung adenocarcinoma (LUAD) (1,2). Although surgery and chemotherapy provide a significant therapeutic effect in early LUAD, advanced and metastatic LUAD are challenging because of their unresectable characteristics and drug resistance (3). Immune disorders in cancer are considered the main factors that promote the occurrence and development of cancer (4). The immune response stimulated by cancer antigens can lead to the elimination of cancer cells, and the same mechanism can be inhibited to provide a microenvironment suitable for cancer growth (5). Due to the lack of blood supply, growing tumors often exist in hypoxic conditions (6). By comparing 38 tumor responses to hypoxia with healthy cells, we found that tumor cells automatically initiate a range of adaptive behaviors (such as angiogenesis, proliferation, and invasion) that ultimately contribute to a more aggressive tumor phenotype (7). A growing body of evidence suggests that there is a direct or indirect interaction between hypoxia and the immune state in a variety of tumor microenvironments (TMEs) (8-10). Therefore, it is necessary to develop new molecular markers by integrating immune, hypoxia, and other influencing factors, which will be more conducive to the accurate diagnosis and effective treatment of LUAD.

ARHGAP11A is an uncharacteristic Rho GTPase activating protein (RhoGAP) located in the plasma membrane at the early stage of mitosis and in the equatorial membrane at the late stage. RhoGAP usually connects cell migration and proliferation pathways that are often down-regulated in cancer (11,12). However, recent studies have found that ARHGAP11A belongs to the RhoGAP family, and plays an opposite role in cancer. ARHGAP11A regulates the proliferation, migration, and invasion of hepatocellular carcinoma (HCC) cells *in vitro* and *in vivo* as well as the development of epithelial-mesenchymal transition (EMT) through ARHGAP11A/Rac1b pathway (13), ARHGAP11A promotes the migration and invasion of cancer cells by inhibiting the reactivation of RhoA and Rac1 (14). Therefore, the molecular mechanism involved in the RhoGAP regulatory network is relatively complex. However, there is an abundance of literature reporting that ARHGAP11A tends to indicate poor prognosis of patients (15). However, the effect of *ARHGAP11A* expression on hypoxia and immune cells is unclear and further studies are needed to reveal its specific role.

The Cancer Genome Atlas (TCGA), Gene Expression Omnibus (GEO), the University of Alabama at Birmingham Cancer (UALCAN), Clinical Proteomic Tumor Analysis Consortium (CPTAC), and Human Protein Atlas (HPA) databases were used to comprehensively analyze the transcriptional level, protein level, prognosis, and clinical significance of *ARHGAP11A* in LUAD. Our study showed that *ARHGAP11A* was abnormally expressed in tumors, closely related to the overall survival of LUAD patients, and represented a newly discovered multifunctional oncogene, which was closely related to hypoxia, immune environment, and hypermutation. Meanwhile, blocking *ARHGAP11A* can effectively inhibit the expression of the programmed cell death ligand 1 (PDL1) and is positively correlated with hypoxia-inducible factor 1α (*HIF1A*) and its downstream proteins vascular endothelial growth factor A (VEGFA) and lactate dehydrogenase A (LDHA) in a hypoxic environment, which presents a more comprehensive rationale and development direction for the treatment of LUAD through ARHGAP11A in the future. We present this article in accordance with the TRIPOD and MDAR reporting checklists (available at https://tcr.amegroups.com/article/view/10.21037/tcr-24-224/rc).

Highlight box

Key findings

- *ARHGAP11A* is closely related to immune and hypoxia in lung adenocarcinoma (LUAD), and can promote the further occurrence and development of tumors.

What is known and what is new?

- Related reports indicate that high expression of *ARHGAP11A* is detrimental to the prognosis of LUAD.
- In this study, we found that *ARHGAP11A* can effectively mediate hypoxia and immune escape in LUAD.

What is the implication, and what should change now?

- The regulation of the tumor microenvironment by *ARHGAP11A* is often multifaceted, especially in terms of immunity, hypoxia, and prognostic development, which presents a new perspective for the treatment of future cancer patients.

Methods

Data sources

The transcriptome data and clinicopathological features of LUAD patients were obtained from TCGA database,

including 59 cases in the normal group and 535 cases in the tumor group. Age, sex, clinical stage, T stage, M stage, N stage, disease-specific survival (DSS) record, and disease-free interval (DFI) were selected as a clinicopathological index of LUAD from clinical information. Mutation data were also included for LUAD patients. GSE115002 and GSE13213 were downloaded from the GEO, including 52 cancer and adjacent tissues and 117 patients with survival time and state, respectively. Then, the protein immunohistochemistry was also downloaded from the HPA database, including 3 normal groups and 6 tumor groups. From the tumor immune estimation resource (TIMER) database, the immune infiltration data and related genes were downloaded and calculated by Cell-type Identification by Estimating Relative Subsets of RNA Transcripts (CIBERSORT) on TCGA-LUAD. The study was conducted in accordance with the Declaration of Helsinki (as revised in 2013).

Screening of differentially expressed genes (DEGs)

Based on the Wilcoxon signed-rank test of the R package, the DEGs between the normal group and tumor group in the TCGA database were made, and the screening threshold was $|\text{LogFC}| \geq 2$, false discovery rate (FDR) <0.05.

Univariate Cox regression analyses

Univariate Cox regression analysis was performed using the DEGs of the TCGA database, and the screening threshold was P<0.0001.

Protein-protein interaction (PPI) network construction and analysis

PPI network analysis was performed using the Search Tool for the Retrieval of Interacting Genes (STRING) database (https://string-db.org); combined scores >0.4 were considered statistically significant. Cytoscape (version 3.4.0) is an open-source bioinformatics software platform for visualizing molecular interaction networks. The top 10 genes were defined according to the high degree of connectivity in the STRING network.

Protein and messenger RNA (mRNA) levels of ARHGAP11A in normal and tumor groups

To verify the protein and mRNA levels of *ARHGAP11A* between normal and tumor groups, the different expressions of TCGA and GEO data in the normal-tumor group were analyzed by R language (r version 4.0.3; R Foundation for Statistical Computing, Vienna, Austria), Wilcoxon signed-rank test, and "limma" package; the screening threshold was $|\log_2 FC| > 1$ and FDR <0.05. Image J software (National Institutes of Health, Bethesda, MD, USA) was used to compare the average optical density (AOD) of immunohistochemistry between the normal group and tumor group in the HPA database, whereby the higher the AOD, the higher the protein content.

ARHGAP11A and clinicopathological features

Kaplan-Meier survival analysis was performed in the high and low expression groups of *ARHGAP11A* from TCGA and GSE13213 datasets, based on the survival package in R language. At the same time, the prognostic analysis of progression-free interval (PFI), DFI, and DSS was studied with the same method for the high and low expression groups of *ARHGAP11A* from TCGA. Then, the receiver operating characteristic (ROC) curve was used to evaluate the accuracy *ARHGAP11A* gene for 1-, 2-, and 3-year prognosis survival. We analyzed the distribution level of *ARHGAP11A* under different clinical characteristics in TCGA datasets using the "limma" package in R language. Next, we studied the influence of *ARHGAP11A* expression level and different clinical factors on the prognosis of patients, based on univariate and multivariate Cox regression analyses. We predicted the 1-, 2-, and 3-year survival probability of patients by drawing a nomogram, and then used the calibration curve to evaluate the nomogram calibration. Overlapping of the actual line with the reference line was taken to indicate that the model has perfect consistency with the actual observation.

Relationship between immune microenvironment and target gene

We downloaded the CIBERSORT score of TCGA-LUAD from the time database and calculated the distribution of immune cell invasion under *ARHGAP11A* high and low expression groups through the R package, and the association between expression level immune cell composition and immune-related genes. Then, we also estimated the immune and matrix scores of LUAD, which was in the TCGA database through the R package "estimate"; at the same time, the correlation between the immune score and the gene expression level was analyzed.

Table 1 Interference sequence information

Fragment name	Sequence (5'-3')
Si-ARHGAP11A-1	GUCCGUCAGAAGAAUUAAUTT
Si-ARHGAP11A-2	GGGCCUUCUAUGGUAUUAATT
Si-ARHGAP11A-3	GCAGCAAUCUUGCAGUAAUTT

Table 2 Antibody information

Antibody name	Source	Number
MMP2	Cell Signaling Technology	13132S
MMP9	Cell Signaling Technology	13667S
CyclinD1	Cell Signaling Technology	55506S
CyclinE1	Cell Signaling Technology	20808S
AKT	Cell Signaling Technology	9272S
P-AKT	Cell Signaling Technology	4060S
PI3K	Cell Signaling Technology	4249S
P-PI3K	Cell Signaling Technology	17366S
HIF1A	Proteintech	20960-1-AP
VEGFA	Proteintech	19003-1-AP
LDHA	Proteintech	19987-1-AP
ARHGAP11A	Affinity Biosciences	DF4425

MMP2, matrix metalloproteinase 2; MMP9, matrix metalloproteinase 9; HIF1A, hypoxia-inducible factor 1A; VEGFA, vascular endothelial growth factor A; LDHA, lactate dehydrogenase A.

Gene set enrichment analysis (GSEA)

GSEA is a calculation method. The expression of *ARHGAP11A* mRNA is divided into high and low expression groups. Then, the datasets h.all.v7.4.symbols.gmt were downloaded from the MSigDB of the GSEA website (https://software.broadinstitute.org/GSEA/msigdb), and the gene enrichment analysis of *ARHGAP11A* was carried out by GSEA4.0 software. The screening parameters were set as the default values for the conditions for significant enrichment.

Enrichment analysis of Gene Ontology (GO) and Kyoto Encyclopedia of Genes and Genomes (KEGG) function

Based on the Database for Annotation, Visualization, and Integrated Discovery (David; (https://David-d.ncifcrf.gov), GO enrichment analysis was performed in the high and low expression groups of *ARHGAP11A*, with $P<0.05$ considered indicative of statistical significance.

Cell culture

A549 and H1299 cell lines from LUAD cell lines were purchased from the American Type Culture Collection (ATCC, Manassas, VA, USA) cell bank and stored in the laboratory in a –196 ℃ liquid nitrogen tank. The complete culture medium was composed of GIBCO 1640 medium (Gibco, Carlsbad, CA, USA), 10% South American fetal bovine serum (BI), and antibiotics (100 μg/mL penicillin and 100 μg/mL streptomycin); they were cultured in a humid air incubator at 37 ℃ and 5% CO_2.

Screening of small interfering RNA (siRNA)

Four pairs of siRNAs designed by Shanghai Gemma Medical Technology (Shanghai, China) were used to interfere with the *ARHGAP11A* gene expression in LUAD cell lines. One group was with empty siRNA without any target gene, and the related sequences were siRNA with different interference efficiency, the related sequences are shown in the *Table 1*. The siRNA with the highest interference efficiency was screened by Western blot analysis.

Western blot analysis

In the radio-immunoprecipitation assay (RIPA) buffer supplemented with protease and phosphatase inhibitors, the cells were rinsed with phosphate-buffered saline (PBS) lysate until the extraction was completed. The protein samples were separated on 10% sodium dodecyl sulfate-polyacrylamide gel electrophoresis (SDS-PAGE), and transferred to the polyvinylidene fluoride (PVDF) membrane (Beyotime Biotechnology, Haimen, China). With the ARHGAP11A, β-tubulin and other monoclonal antibodies (1:3,000) were incubated overnight, washed three times, and rabbit secondary antibodies (1:1,000) were incubated for 1 hour. The results of Western blot analysis were analyzed by the image analysis software. The specific antibody source information is shown in *Table 2*.

Cell proliferation test

The proliferation ability of lung cancer cells after interference was evaluated by the plate cloning method and 3-(4,5-dimethyl-2-thiazolyl)-2,5-diphenyl-2H-tetrazolium bromide (MTT) method. After planting cells on a six well

plate overnight, negative and *ARHGAP11A*-interference (NC and Si3) treated cells were added for eight hours. The supernatant was discarded, digested, and the cells were centrifuged before being blown into a cell suspension. The different groups of cell suspensions were injected into a six-well plate with a density of 1,000 cells per plate, incubated for 7 days, and finally the number of colonies was counted. Then, 1,000 cells from different groups of cell suspensions were plated in each well of 96 well plates and incubated with MTT reagent overnight. The absorbance at 490 nm was measured by a microplate reader.

Cell migration and invasion test

The migration of lung cancer cells was tested by Transwell and scratch test: 200 μL serum-free single-cell suspension was injected into the Transwell chamber, and the number of cells per well was maintained at 4×10^4. After incubation for 24–48 hours, the chamber was taken out, cleaned with PBS, fixed with 4% paraformaldehyde, and then treated with 500 μL crystal violet stain in the Transwell chamber for 5 minutes. Finally, six visual field cells were observed under the microscope and photographed and counted to detect cell migration and invasion by the Transwell method. During the scratch test, each group of cells was inoculated into a six-well plate, and the number of cells reached 70–80% after incubation for 48 hours. Three scratches were made in each well. The scratch areas were photographed with a microscope at 0, 12, and 24 h respectively. The scratch healing area was calculated by the following formula: scratch healing (%) = (initial scratch area-final scratch area)/initial scratch area ×100%. During cell invasion, Matrigel (Corning, Shanghai, China) was evenly coated in the Transwell upper chamber, left in the 37 ℃ incubators for about 40 minutes, and solidified naturally. The other steps were the same as those in the Transwell migration experiment.

Cell cycle assay

Cells were planted overnight in a six well plate (3×10^5 cells/well) and incubated in a mixture of LiP2000 and SiRNA (NC and Si3) for 6–8 hours. The supernatant was discarded and added to normal culture medium for 36 hours. Then, the cells were collected, fixed in 70% ethanol overnight, stained with propidium iodide (PI)/RNase A solution (Cell Cycle and Apoptosis Analysis Kit, Beyotime Biotechnology), and maintained at 37 ℃ for 30 minutes. The fluorescence was collected between 620 and 650 nm by flow cytometry. Finally, the cell ratios of G0/G1, S, and G2/M phases were calculated.

Analysis of apoptosis by flow cytometry

Cells were cultivated to the sixth power of approximately 4×10^5 in a six well plate, and after 48 hours of interference treatment (NC and Si3), adherent lung cancer cells were digested with 0.25% trypsin without ethylenediaminetetraacetic acid, and then centrifuged at 1,500 rpm for 5 minutes to collect the supernatant. Then, the collected cells were washed with precooled PBS three times. Annexin V staining was performed with annexin V-fluorescein isothiocyanate (FITC) apoptosis detection kit (Beyotime Biotechnology) according to the manufacturer's protocol, and FACScalibur, or FACSCanto instrument (Becton Dickinson, and Co., Franklin Lakes, NJ, USA) was used to analyze the apoptosis rate by flow cytometry.

Lactic acid and glucose experiment

The cells were seeded on a six well plate (3×10^5 cells/well) overnight and subjected to knockdown treatment for 36 h. The supernatant was discarded from each group and added to the same basic culture medium for cultivation for six hours. The supernatant was then aspirated for later use, and the lactate and glucose levels in different treatment groups were measured using lactate and glucose assay kits (Sigma-Aldrich, St. Louis, MO, USA).

Statistical analysis

Based on R language, various software packages such as "limma", "survival", and "ggplot" are used for statistical analysis and plotting of public data. Graphpad Prism 8.0 (GraphPad Software, San Diego, CA, USA) was used for statistical analysis and plotting of cell function experiments, and commonly used statistical methods included Student's *t*-test or Wilcoxon test.

Results

Screening of immune and hypoxia-related core gene ARHGAP11A

First, 2,748 DEGs were obtained from both normal and tumor groups in the TCGA database (*Figure 1A*,*1B*), about 2,498 immune-related genes were downloaded from the TIMER website, and the immune core genes with an

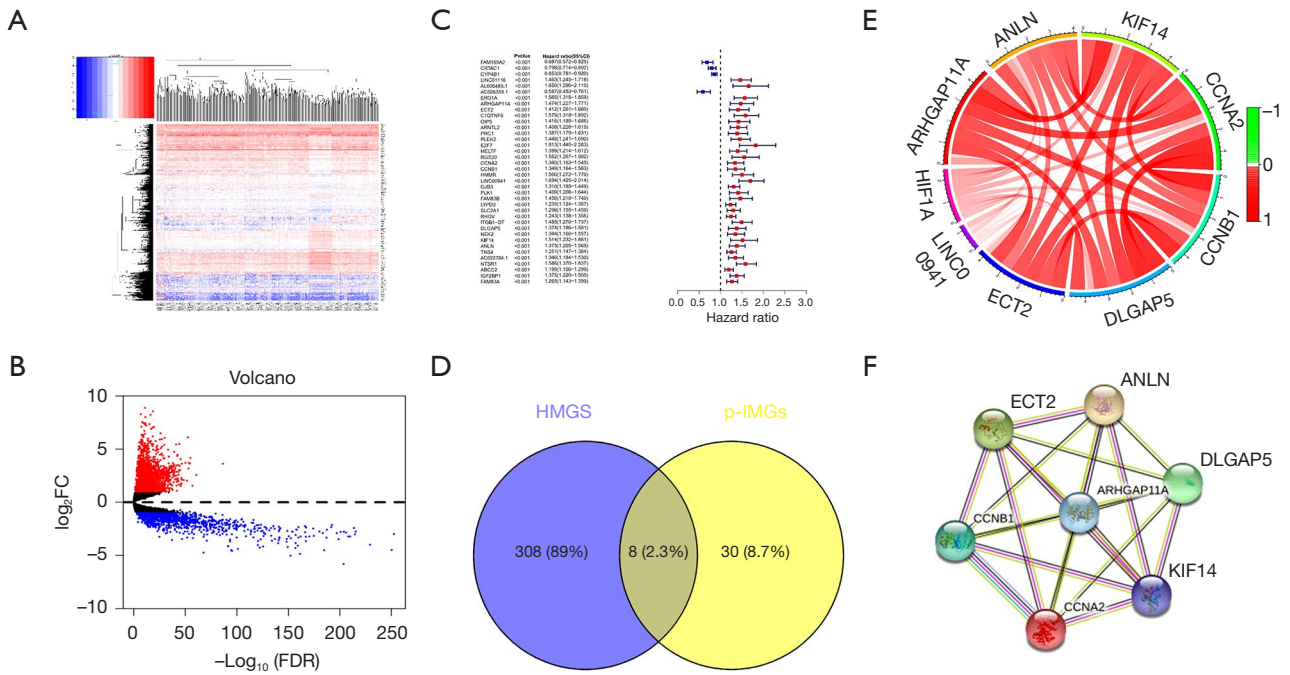

Figure 1 *ARHGAP11A* is a core gene related to immunity and hypoxia in LUAD. (A) Heat map and (B) volcano map of differentially expressed genes in LUAD (red dots: genes with high expression in tumors; black dots: genes with insignificant tumor differences; blue dots: genes with low expression in tumors). (C) Forest plot of hazard ratios showing the prognostic values of immune-related genes. (D) Wayne diagram of intersection of immune and hypoxia-related genes. (E) Heat map of correlation between 8 key genes and HIF1A. (F) A protein-protein interacting network of 7 key genes. LUAD, lung adenocarcinoma; FC, fold change; FDR, false discovery rate; HMGS, HIF1A-related genes; p-IMGs, 38 prognosis-associated immune core genes; CI, confidence interval.

immune-related gene correlation coefficient of 0.4 (P<0.05) were screened from the DEGs. A total of 38 prognosis-associated immune core genes (p-IMGs) were obtained (*Figure 1C*) using univariate Cox regression analysis (P<0.001). A total of 316 *HIF1A*-related genes (HMGS) with a *HIF1A* correlation coefficient of 0.4 (P value <0.05) were filtered from the immune core genes. Then, eight immune and hypoxia-related-prognostic genes (P-HIMGS) were obtained by the intersection of 316 HMGS and 38 p-IMGs (*Figure 1D*). Through the STRING online database, among the PPI networks of 7 P-HIMGS, *ARHGAP11A* had the most relevant nodes and the highest correlation coefficient with *HIF1A* (*Figure 1E,1F*).

Expression of ARHGAP11A in LUAD

We downloaded the gene expression dataset of GSE115002 (P<0.001) from the GEO database (*Figure 2A*). *ARHGAP11A* gene expression was also significantly increased in the tumor group compared to different groups. The immunohistochemical-related samples and expression level of ARHGAP11A protein were downloaded from the HPA database and CPTAC analysis in UALCAN; compared with the normal group, the ARHGAP11A protein level in cancer tissue was significantly increased (P<0.001) (*Figure 2B-2D*).

The protein expression of ARHGAP11A was higher in tumor cells

We found that after BEAS-2B, A549, and H1299 cells had been cultured in a cell incubator at 37 ℃ and 5% CO_2 for 2 days, the expression of ARHGAP11A in the extracted protein was higher in A549 and H1299 cells (*Figure 2E*).

The prognostic impact of ARHGAP11A on LUAD patients

Based on median of *ARHGAP11A* expression, the high

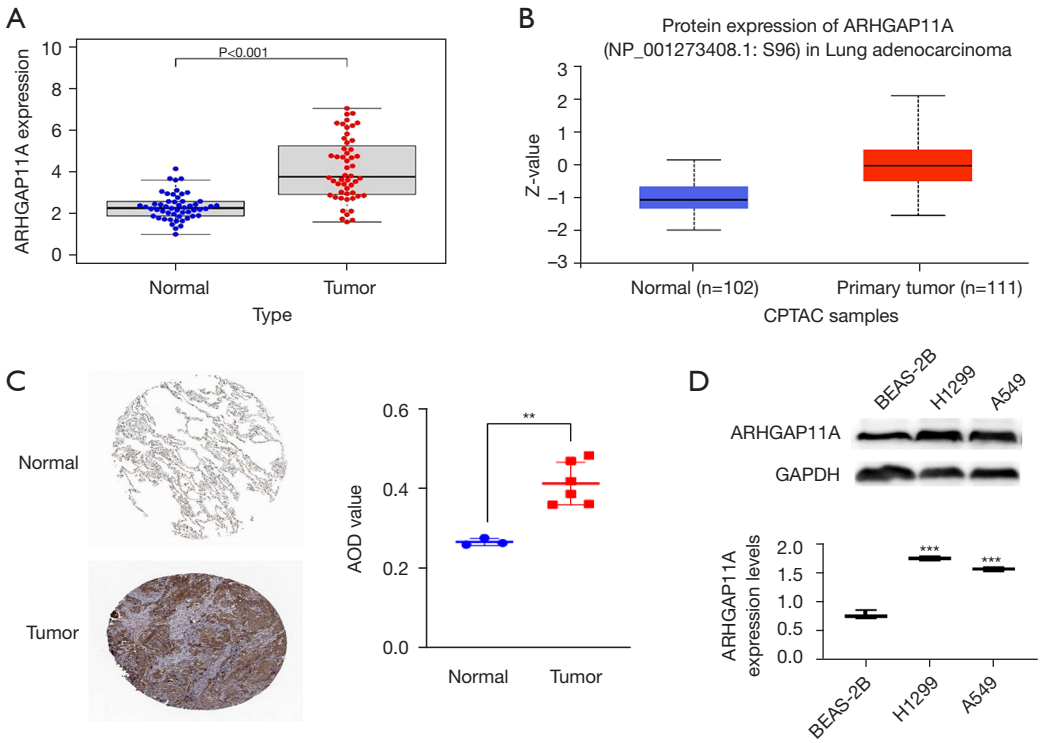

Figure 2 *ARHGAP11A* is highly expressed in lung adenocarcinoma. (A) *ARHGAP11A* showed prominently high expression in tumor tissue than in non-cancerous tissues based on Wilcoxon rank-sum test from GEO database. (B) The protein expression levels of ARHGAP11A based on CPTAC. (C) Validation of protein expression levels of ARHGAP11A in the HPA database. Tumor tissue, https://www.proteinatlas.org/ENSG00000198826- ARHGAP11A/pathology/lung+cancer#img; normal tissue, https://www.proteinatlas.org/ENSG00000070193-FGF10/tissue/lung#img. (D) Expression of ARHGAP11A in human bronchial epithelial cells (BEAS-2B) and lung adenocarcinoma cells (H1299 and A549) by Western blot and using Image J quantitative analysis software. **, P<0.01; ***, P<0.001. GEO, Gene Expression Omnibus; CPTAC, clinical proteomic tumor analysis consortium; HPA, Human Protein Atlas; AOD, average optical density.

expression group was significantly associated with poor overall survival (OS) (P=0.002), and survival prognosis was poor in patients with high *ARHGAP11A* expression in the GEO dataset (P<0.001) (*Figure 3A,3B*), suggesting that high *ARHGAP11A* expression is detrimental to patient prognosis. ROC curve analysis of TCGA validation set (*Figure 3C*) and GSE13213 test set (*Figure 3D*) was used to evaluate the predictive value of *ARHGAP11A* expression in 1-, 2-, and 3-year survival rates. The area under the curve (AUC) of the TCGA dataset was 0.642, 0.637, and 0.640, while the GEO dataset demonstrated better predictive ability with AUC values of 0.801, 0.706, and 0.745. The barplot indicated that the survival status was worse in patients with higher expression groups in the TCGA cohort (*Figure 3E*), and the GSE13213 cohort (*Figure 3F*). Prognostic factors such as age, sex, stage, tumor, node, metastasis (TNM) stage, and *ARHGAP11A* expression were used to establish nomogram for predicting 1-, 2-, and 3-year survival in LUAD patients (*Figure 3G*). The calibration curve of the nomogram is close to the best prediction curve, C-indexes of the nomogram were 0.702 [95% confidence interval (CI): 0.647–0.757], indicating that the prediction ability of LUAD patients at 1, 2, and 3 years is highly consistent (*Figure 3H-3J*). Other related survival analyses of DSS (P<0.001) (*Figure 3K*), DFI (P=0.03) (*Figure 3L*), and PFI (P=0.02) (*Figure 3M*), also indicate that high expression of *ARHGAP11A* is detrimental to the prognosis of patients.

Correlation between ARHGAP11A and hypoxia regulation

In the high *ARHGAP11A* group, the distribution levels of *HIF1A*, *LDHA*, and *VEGFA* were higher (*Figure 4A-4C*). *ARHGAP11A* was positively correlated with *HIF1A*, *LDHA*, and *VEGFA*, respectively (*Figure 4D-4F*). There was no

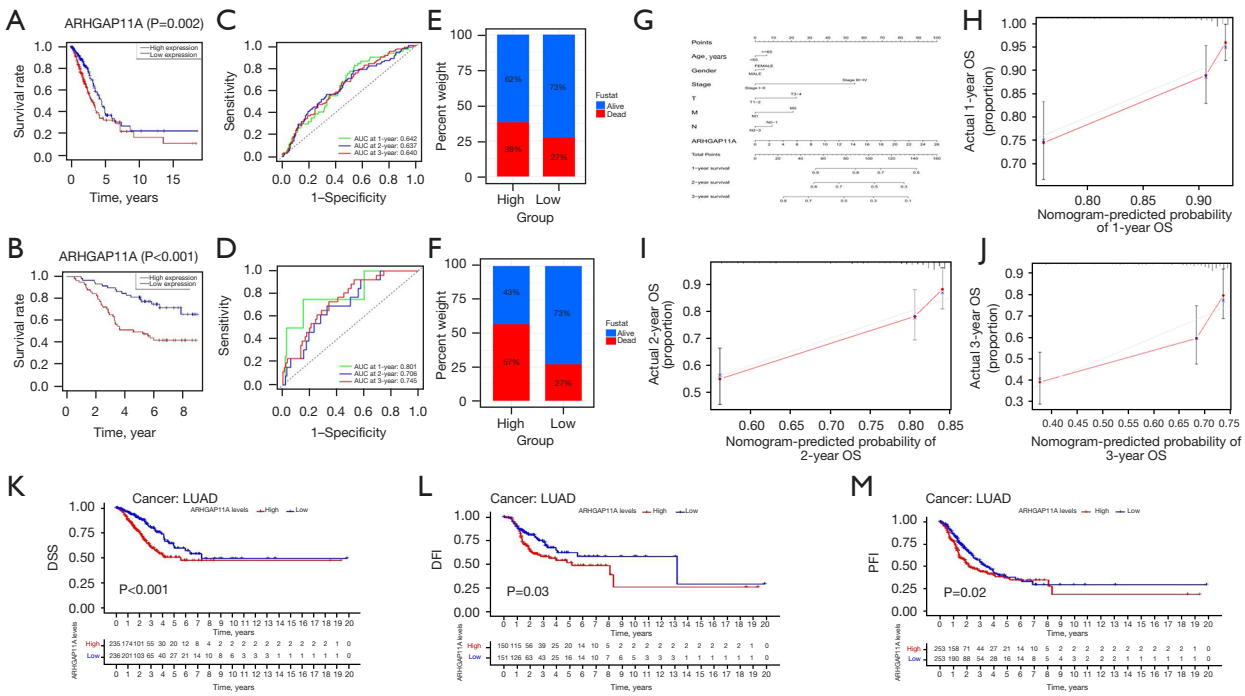

Figure 3 Effect and validation of *ARHGAP11A* expression on prognosis of patients with LUAD. (A-D) The OS time of patients *ARHGAP11A* high and low expression group in TCGA (A) and GEO (B) datasets. ROC curve analysis in the TCGA (C), GEO (D) cohort. The bar plot showed the relationship with the expression of *ARHGAP11A* and survival status in the TCGA cohort (E), GEO cohort (F). (G) The nomogram of independent prognostic factors was constructed to predict the survival probability at 1 year, 2 years and 3 years of LUAD patients. (H-J) The calibration chart shows the prediction ability of the nomogram for 1 years (H), 2 years (I), and 3 years (J). (K) DSS, (L) DFI, (M) PFI. LUAD, lung adenocarcinoma; OS, overall survival; TCGA, The Cancer Genome Atlas; GEO, Gene Expression Omnibus; ROC, receiver operating characteristic; AUC, area under the curve; DSS, disease-specific survival; DFI, disease-free interval; PFI, progression-free interval.

significant difference in prognosis between high and low *ARHGAP11A* in patients with high expression of *HIF1A* (*Figure 4G*). Among the patients with low expression of *HIF1A*, those with high expression of *ARHGAP11A* had a poor prognosis (*Figure 4H*). Under the combined survival analysis of *HIF1A* and *ARHGAP11A*, the prognosis analysis of the two genes had a synergistic effect, and the prognosis of patients with high *HIF1A* and *ARHGAP11A* was the least favorable (*Figure 4I*).

Immune correlation of ARHGAP11A

The CIBERSORT algorithm was used to infer the infiltration of immune cells in the TME of LUAD in the TCGA dataset. LUAD was divided into high and low groups according to the expression of *ARHGAP11A*. We found that the immune invasion of T cells CD8, T cells CD4 memory activated, and macrophages M0 and M1 had a higher proportion in the high expression group. Compared with the low expression group, monocytes, T cells CD4 memory resting, macrophages M2 and dendritic cell activated, B cells memory, and mast cells resting showed a higher proportion (*Figure 5A*). Based on Spearman analysis, the correlation coefficient between *ARHGAP11A* expression and immune cell score was more than 0.25, including macrophages M1 and M0, T cells $CD4^+$ memory activated, and mast cells resting, whereas it was negatively correlated with B cells memory, mast cells activated, and myeloid dendritic cells resting and the correlation coefficient was less than −0.25 (*Figure 5B*). The stromal scores and an immune score of LUAD in TCGA were calculated by using the estimate method in the R package (*Figure 5C,5D*). The results showed that the stromal scores (P<0.001) and immune score (P=0.01) of low the group were significantly higher than the high group. Meanwhile, in GO enrichment

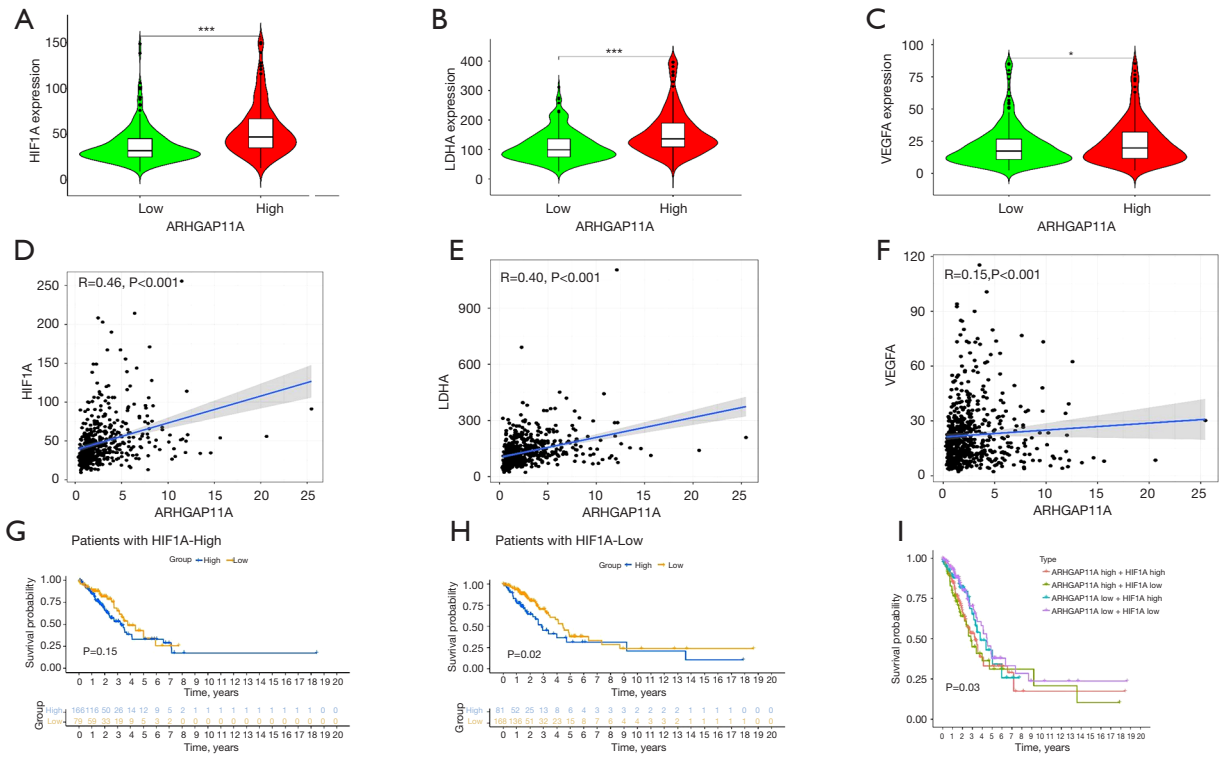

Figure 4 The expression of *ARHGAP11A* is closely related to hypoxia. (A-C) Violin diagram showing that HIF1A (A), LDHA (B), and VEGFA (C) are significantly distributed in the high group than the low group. (D-F) Correlation linear diagram of *ARHGAP11A* with HIF1A (D), LDHA (E), and VEGFA (F), respectively. (G-I) Kaplan-Meier survival analysis of high (G) and low hypoxia groups (H) under different expression groups of *ARHGAP11A*. (I) Combined survival analysis of *ARHGAP11A* and *HIF1A*. *, P<0.05; ***, P<0.001.

analysis of significant genes in the *ARHGAP11A* low expression group, immune-related pathways mainly focused on endogenous lipid antigen binding, receptor-mediated endocytosis, endogenous lipid antigen binding, exogenous lipid antigen binding, and antigen processing, and presentation. Exogenous lipid antigen and immune response were obtained through the MHC IB class. B-lymphocyte antigen CD20, CD23, and IL2 were mainly enriched in the low-expression group (*Figure 5E-5G*), as the immunosuppression was related to PDL1, whereas programmed cell death protein 1 (PD1) and cytotoxic T lymphocyte-associated protein 4 (*CTLA4*) genes were significantly focused in the high-expression group (*Figure 5H-5J*). In addition, *ARHGAP11A*-related survival analysis was performed in high and low expression groups of *PD1*, *CTLA4*, and *PDL1* (*Figure 5K-5P*). We found that *ARHGAP11A* with low expression had a better prognosis in the *PDL1* and *CTLA4* high expression group and the *PD1* low expression group (*Figure 5L,5M,5O*).

Enrichment analysis of the GO function

The DEG expression was analyzed in the high and low expression group of *ARHGAP11A* using R software (FDR =0.05, $|\log_2 FC|$ =2) (*Figure 6A*). Based on the David online analysis website, KEGG and GO functional enrichment analysis of significant genes in the high- and low-expression groups, it was found that the low expression group was mainly enriched in immune-related pathways, including endogenous lipid antigen binding, exogenous lipid antigen binding, antigen processing and presentation, exogenous lipid antigen via MHC class Ib, immune response, complement, and coagulation cascades (*Figure 6B*) and the high expression group was mainly enriched in innate immune response in mucosa, positive regulation of innate immune response, regulation of cytokine biosynthetic process, cellular response to hypoxia, defense response to Gram-positive bacterium, DNA damage response, detection of DNA damage, and leukocyte

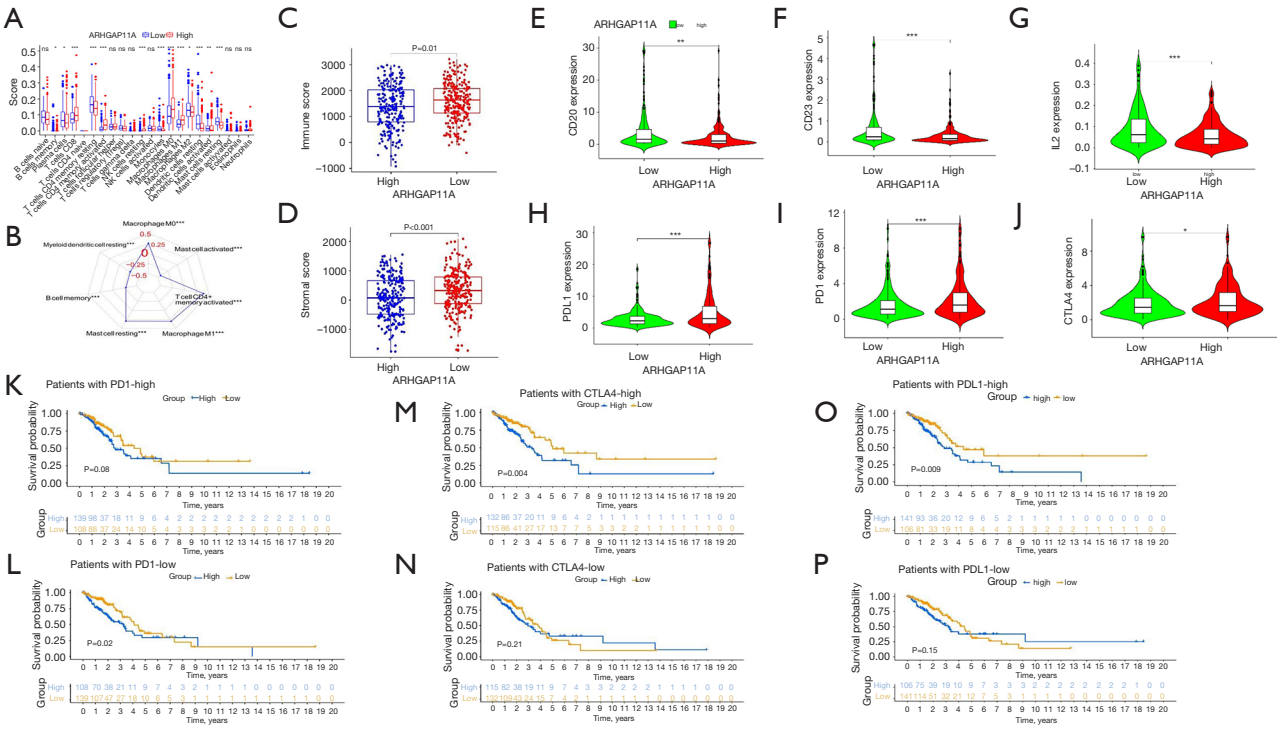

Figure 5 Correlation analysis of the expression of *ARHGAP11A* and immune cell infiltration. (A) Differences of 22 immune cell subtypes between high and low expression groups of *ARHGAP11A*. (B) Radar chart showing the correlation between the high and low expression of *ARHGAP11A* and the degree of invasion of immune cells infiltration. (C) Immune score and stromal score (D) in the high and low expression group of *ARHGAP11A*. (E-J) Violin diagram shows the expression levels of CD20 (E), CD23 (F), IL2 (G), PDL1 (H), PD1 (I), and CTLA4 (J) in different groups. (K-P) Survival analysis of different expression groups of *ARHGAP11A* under high and low expression group of PD1 (K,L), CTLA4 (M,N), PDL1 (O,P). ns, no statistical significance; *, P<0.05; **, P<0.01; ***, P<0.001. IL2, interleukin-2; PDL1, programmed cell death ligand 1; PD1, programmed cell death protein 1.

chemotaxis involved in inflammatory response (*Figure 6C*).

GSEA analysis of ARHGAP11A-related signaling pathways

We analyzed the functional enrichment of the *ARHGAP11A* high- and low-expression groups using the hallmark dataset in the GSEA tool and found that the high expression group was mainly enriched in PI3K/AKT/mTOR pathway, glycolysis, and hypoxia (*Figure 6D-6F*).

Screening of the best interference sequence

We verified the knockout efficiency of the three groups of interference sequences by Western blot. The results showed that the interference sequence 3 could knock down the protein expression level of ARHGAP11A in H1299 and A549 cells to the greatest extent (*Figure 7A,7B*).

Cell proliferation test and plate cloning experiment

MTT colorimetry was used to detect the proliferation activity of A549 and H1299 cells. We found that the optical density (OD) value measured at 490 nm in the interference group decreased continuously from 24 to 72 h (*Figure 8A,8B*). After the tumor cells in the interference and NC group were cultured in the incubator for 7 days, the cell spots in the interference group decreased significantly (*Figure 8C,8D*).

Glucose and lactate content experiment

After 36 hours of interference with cell treatment, the cell supernatant was collected and the amount of lactate and glucose production was measured using a glucose and lactate assay kit. We found that in tumor cells, knocking down *ARHGAP11A* resulted in a significant decrease in lactate levels, whereas the effect on glucose content was the opposite (*Figure 8E,8F*).

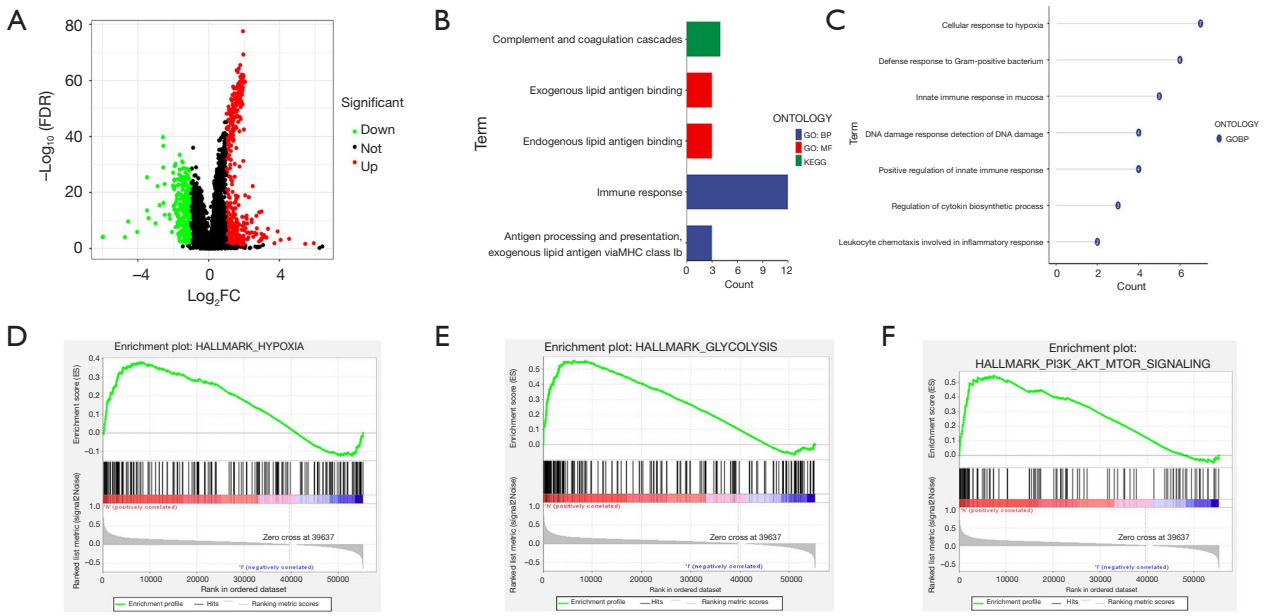

Figure 6 KEGG and GO enrichment analysis of DEGs in high and low expression groups of *ARHGAP11A*. (A) Volcano plot of differentially expressed genes. (B,C) The results of immune and hypoxia-related KEGG and function analysis of differentially expressed genes in the low (B) and high (C) expression group. (D-F) The significant genes in the increased expression group were mainly enriched in the hypoxia (D), glycolysis (E), and PI3K/Akt/mTOR (F) signal pathways, via the Hallmark dataset in GSEA. KEGG, Kyoto Encyclopedia of Genes and Genomes; GO, Gene Ontology; DEGs, differentially expressed genes; GSEA, gene set enrichment analysis; FC, fold change; FDR, false discovery rate.

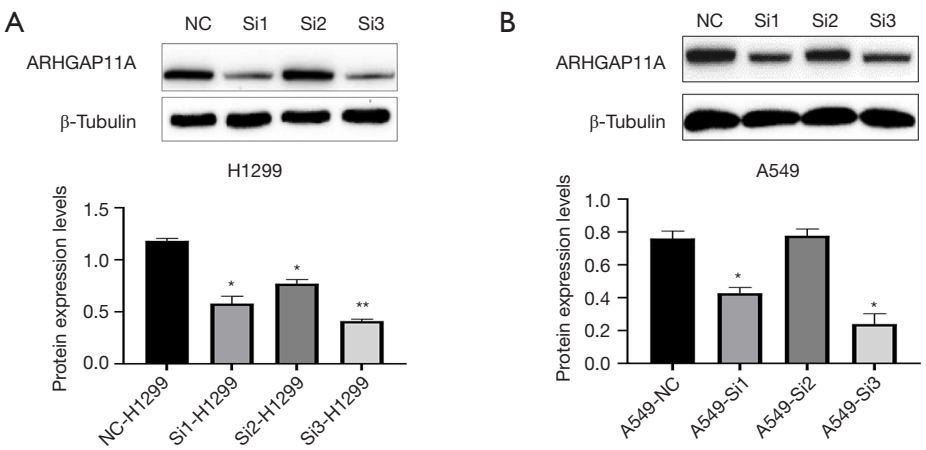

Figure 7 Screening for the most efficient small interfering RNA. (A) H1299. (B) A549. *, P<0.05; **, P<0.01.

Cell migration and invasion test

In the Transwell experiment, the number of migrating and invasive cells in the *ARHGAP11A* group was significantly lower than that in the NC group (*Figure 9A,9B*). In the scratch experiment, the migration speed of the knockdown group significantly decreased (*Figure 9C,9D*).

Apoptosis and cell cycle

The total apoptosis rate of A549 and H1299 cells in the interference group was significantly higher than that

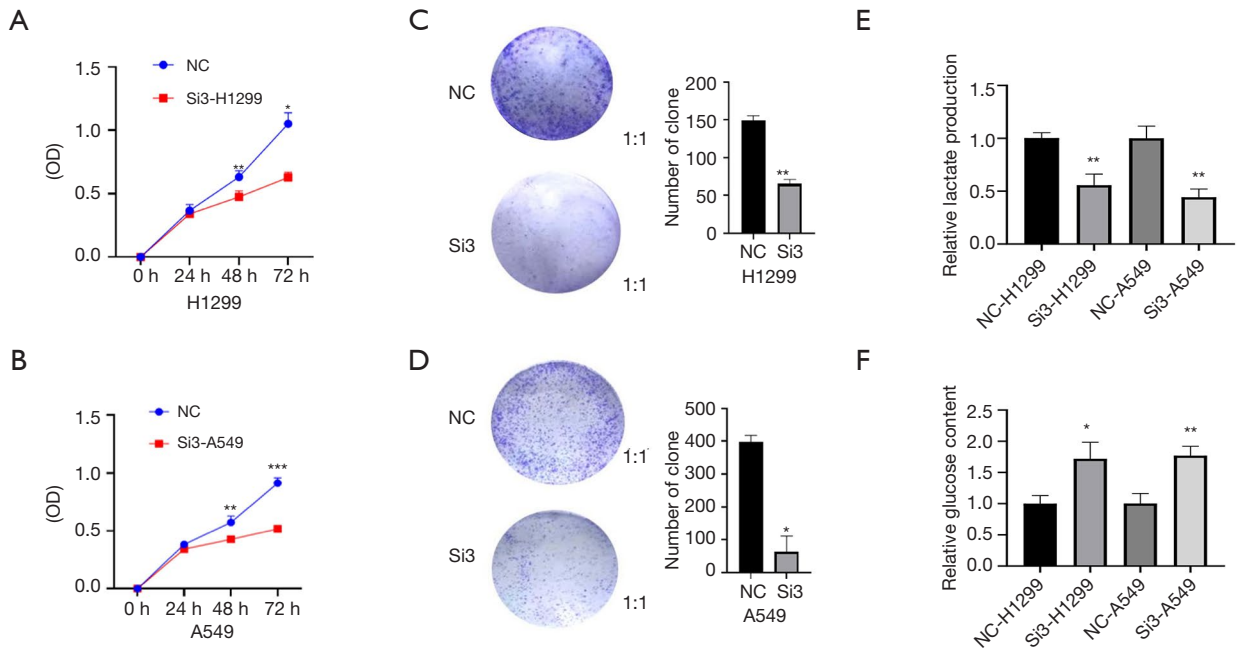

Figure 8 Suppression of *ARHGAP11A* can inhibit the proliferation of A549 and H1299 cells. (A-D) MTT assay and plate cloning experiment (crystal violet staining). (E,F) Lactic acid and glucose determination experiment. *, P<0.05; **, P<0.01; ***, P<0.001. MTT, 3-(4,5-Dimethyl-2-thiazolyl)-2,5-diphenyl-2H-tetrazolium bromide; OD, optical density.

in the normal group (*Figure 10A,10B*). In H1299 cells, compared with the NC group, the interference group mainly stagnated in the G0/G1 phase and decreased in the S phase. In addition, in A549 cells, the interference group also mainly stagnated in the G0/G1 phase and decreased in the S phase (*Figure 10C,10D*).

In the interference group, the changes of cycle, apoptosis, migration, and proliferation proteins were observed. After reducing the protein expression of *ARHGAP11A*, the anti-apoptotic protein BCL2 decreased and the pro-apoptotic proteins BAX and Caspase-3 increased. Decreased proteins, including cell cycle protein E1, D1 (CyclinD1, CyclinE1), matrix metalloproteinase 2 and 9 (MMP2, MMP9), and P-phosphatidylinositol 3-kinase and protein kinase B (P-PI3K and P-AKT) remained unchanged (*Figure 11A,11B*).

Knockdown of ARHGAP11A decreased the expression of PDL1 in A549/H1299 cells

After the knockdown of *ARHGAP11A* by the best small disruptor, the expression of PDL1 decreased in LUAD A549/H1299 cells (*Figure 12A,12B*).

Hypoxia injury of LUAD cell line A549/H1299 induced by CoCL2

After 24 hours of CoCL2-induced LUAD, the HIF1A factor increased significantly in the treatment group compared with the blank group according to Western blot analysis (*Figure 12C*).

Under hypoxic conditions, knockdown of ARHGAP11A decreased the expression of HIF1A, VEGFA, and LDHA in A549 H1299 cells

After CoCL2-induced hypoxic injury of LUAD cells and establishment of a hypoxic microenvironment, it was found that HIF1A, VEGFA, and LDHA decreased by knocking down the expression of *ARHGAP11A* in tumor cells (*Figure 12D*).

Discussion

The RhoGAP family is characterized by the RhoGAP domain composed of 150 amino acids, which can bind and stimulate with guanosine triphosphate (GTP)-loaded Rho GTPase (16,17). Rho GTPase is the main regulator

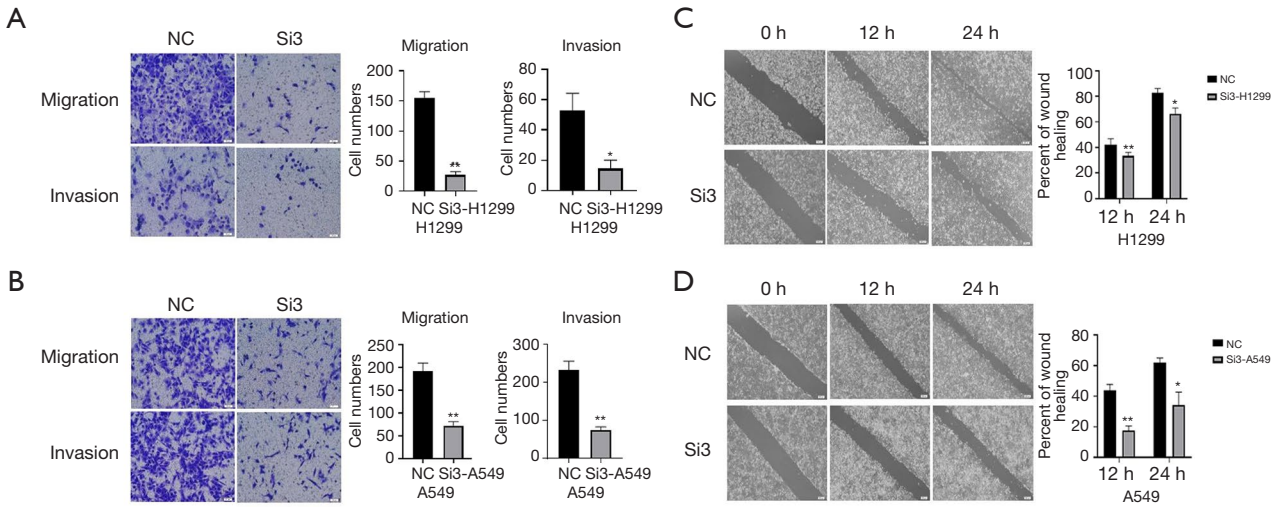

Figure 9 Knocking down the expression of *ARHGAP11A* affects migration and invasion of tumor cells H1299 and A549. (A-D) Migration and invasion of tumor cells demonstrated through Transwell and scratch experiments [(A,B) Representative images of crystal violet staining, Micrographs captured by transmission electron microscopy. Scale bars: 50 μm (A,B) and 200 μm (C,D)]. *, P<0.05; **, P<0.01.

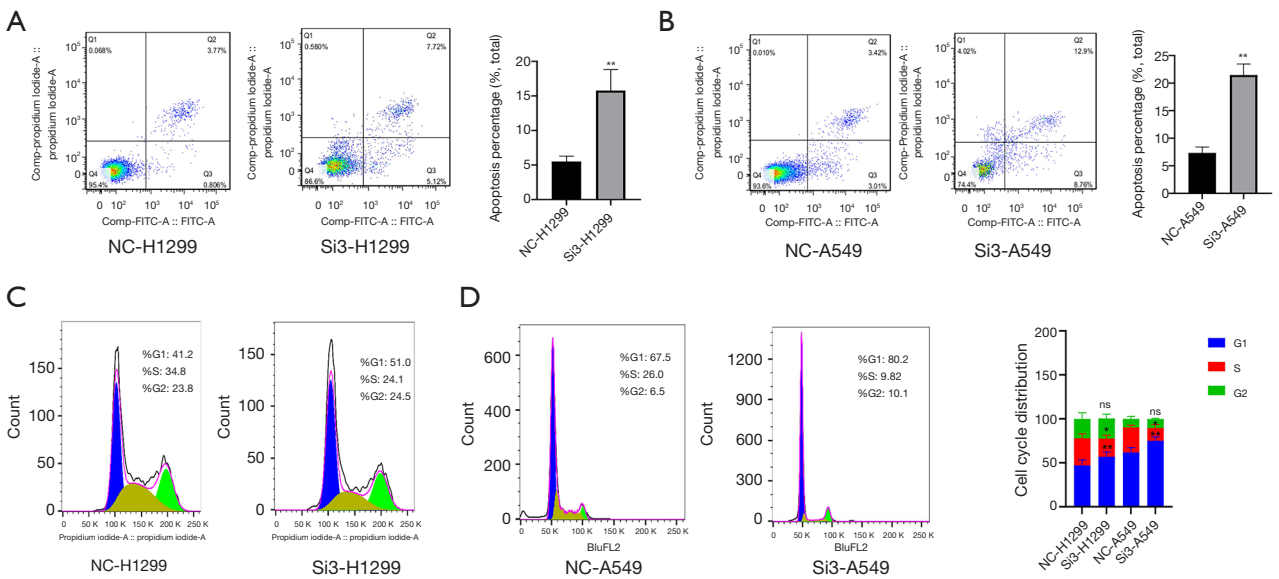

Figure 10 Inhibiting the expression of *ARHGAP11A* can promote the apoptosis of tumor cells and hinder the conversion of G1/S phase. (A,B) Flow cytometry apoptosis test. (C,D) Flow cycle experiment (blue represents G1 phase, brown represents S phase, and green represents G2 phase; the black lines in the periodic chart represent the lines of each cycle, whereas the red lines represent the results of peak correction and fitting for each cycle). *, P<0.05; **, P<0.01; ns, no statistical significance.

of the actin cytoskeleton during cell migration, but it also plays an important role in microtubule dynamics, membrane transport, proliferation, gene expression, and cell differentiation (18,19). On account of these pleiotropic functions, Rho GTPase is involved in many pathological conditions, such as cancer (17). A gene family encoding the Rho gap (archtop) turns off Rho-like GTPase (16,20). Recently, studies on the RhoGAP family have found that most of them are tumor suppressors, such as *DLC1* (21), the anti-tumor effect of ARHGAP25

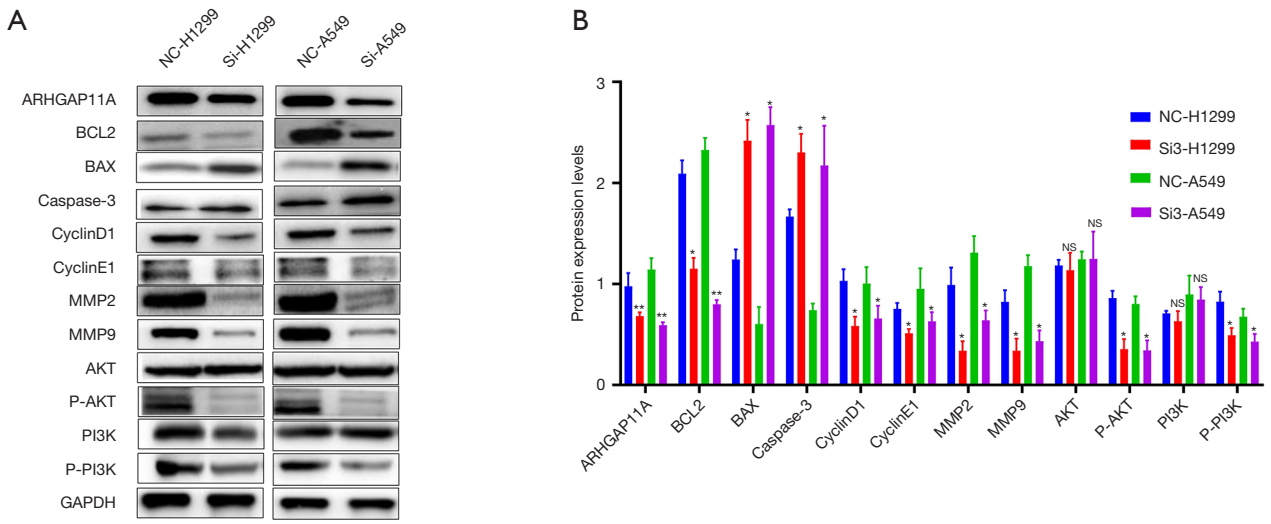

Figure 11 The expression level of related proteins in interference and control groups. (A,B) Cycle associated protein (CyclinE1, CyclinD1), Apoptosis protein (BCL2, BAX, and Caspase-3), migration and invasion proteins (MMP2 and MMP9), proliferative protein (PI3K and AKT). *, P<0.05; **, P<0.01; NS, no statistical significance.

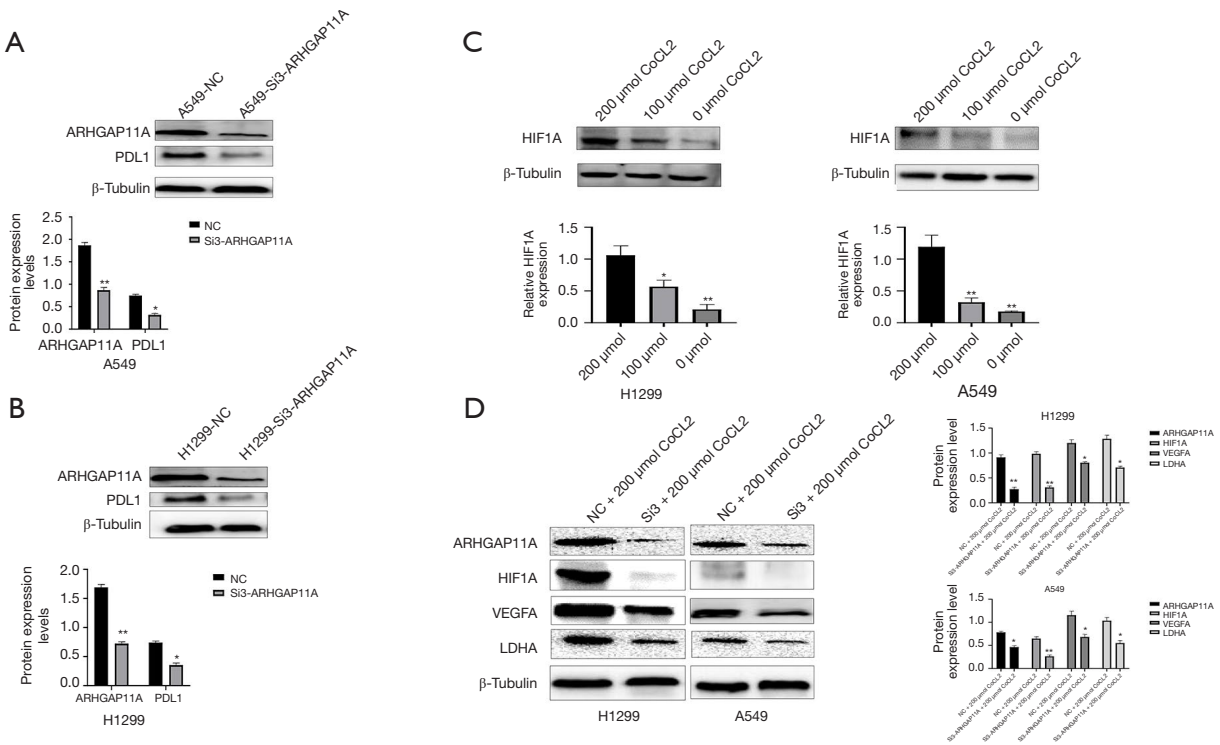

Figure 12 After interfering with the expression of *ARHGAP11A*, the modification of an immune-related protein, and the changes of hypoxia-inducible factors and regulatory factors after CoCL2 induced hypoxia. (A,B) After the knockdown of *ARHGAP11A*, the expression levels of PDL1 in A549 (A) and H1299 (B) cells, were determined by Western blot. (C) After 0, 100, and 200 μmol CoCL2 induction, the expression of HIF1A in A549 and H1299 cells was detected by Western blot. (D) After 200 μmol CoCL2 induction and knockdown of *ARHGAP11A*, the effects on the proteins of HIF1A, VEGFA, and LDHA in H1299 and A549 were detected by Western blot. *, P<0.05; **, P<0.01. PDL1, programmed cell death ligand 1; CoCL2, cobalt chloride.

in lung cancer cells (22), and the decreased expression of *ARHGAP15* promotes the development of colorectal cancer (23). It is also found that this classification does not apply to all members of the Rho gap family, for example, *ARHGAP42* promotes nasopharyngeal carcinoma cell migration and invasion (24), interference with *ARHGAP9* inhibits gastric cancer cell proliferation and EMT (25), *ARHGAP5* promotes colorectal cancer metastasis (26), and *ARHGAP11A* plays a promoting role in a variety of tumors (13-15). However, the specific effects of *ARHGAP11A* gene expression on immune invasion and hypoxia in LUAD have not been reported. In this study, we evaluated the *ARHGAP11A* gene expression profile by bioinformatics analysis using TCGA, GEO, and HPA databases. The expression of the *ARHGAP11A* gene and protein was significantly higher in LUAD patients than in matched normal lung tissue, and those of H1299 and A549 proteins were higher in LUAD cells than in normal BEAS-2B cells.

We also researched the association between *ARHGAP11A* expression and the clinicopathological features and prognosis of LUAD patients, as well as the effect of high *ARHGAP11A* expression on the prognosis of LUAD patients. Our study found that the *ARHGAP11A* was closely correlated with OS, DFI, PFI, and DSS. ROC curve analysis showed that *ARHGAP11A* had a good predictive value for the prognosis of patients within three years. In the current study, age, gender, T, M, N, stage, and *ARHGAP11A* were used to establish nomogram to predict the prognostic risk of LUAD patients. The calibration chart showed that the actual prognosis is very close to the predicted prognosis, which indicates that the nomogram has good predictive performance.

Then, we also analyzed the immune invasion and immune gene correlation of *ARHGAP11A*-high and -low expression groups. Although there was a large number of CD8 T cells in the high expression group, PD1, PDL1, and CTLA4 were at the high expression level. In the past, the high expression of these three genes often inhibited the activation, expansion, and effector function of $CD8^+$ T cells, it also helps cancer cells escape from immune destruction (27) in the TME which is not conducive to anticancer activity. We found that the low group was distributed in large quantities with dendritic cells and CD23-related genes. As previously reported, dendritic cells absorb, process, and present extracellular antigens to $CD8^+$ T cells through MHC-I. This process is also called cross-presentation. It is necessary to activate $CD8^+$ T cells and has a considerable impact on immune monitoring in transplantation and immune defense in infection (28,29). At the same time, B cell and its related genes CD20 and interleukin-2 (IL-2) were also widely distributed in the low expression group, which means that B cells may play a positive role in the prognosis of LUAD, we also found that many articles reported that a large number of B cell invasion is beneficial to the prognosis of a variety of tumors (30,31). Through KEGG and GO pathway analysis on the David online website, the low expression group should be enriched in endogenous lipid antigen binding, exogenous lipid antigen binding, antigen processing and presentation, exogenous lipid antigen via MHC class Ib, immune response, complement, and coagulation cascades, thus it can be further explained that the low expression of *ARHGAP11A* is closely related to B cells and dendritic cells. The expression level of *ARHGAP11A* exhibited a positive correlation with that of hypoxia-inducible factor (HIF). Notably, *ARHGAP11A* was extensively distributed within the high-expression group and was prominently enriched in the cellular response to hypoxia, as demonstrated by the Ingo results. In light of the combined survival analysis of *HIF1A* and *ARHGAP11A*, it was observed that patients with low expression levels of both *HIF1A* and *ARHGAP11A* exhibited the most favorable survival outcome. During hypoxia, tumor cells are more prone to proliferation, metastasis, drug resistance, and poor prognosis (32). *HIF1A* can induce stem cells to survive and expand cancer stem cells (CSCs) (33,34). However, immunotherapy can only bring good benefits to some patients with lung cancer, and many patients still do not achieve the ideal effect after using immune checkpoint inhibitors (35,36). Therefore, we need a new immune molecule-targeted drug to improve the survival time of patients. Through the hallmark dataset in the GSEA resource, the high expression group was shown to be mainly enriched in PI3K/AKT/mTOR, glycolysis, and hypoxia signaling pathway. In previous studies, the activation of the PI3K/AKT/mTOR signal plays a crucial role in promoting tumorigenesis, the development of cancer is promoted through various mechanisms. Therapeutic inhibition of the PI3K/AKT/mTOR signaling network may prevent the activation of the immunosuppressive pathway, enhance the inherent characteristics of anti-tumor immunity, and enhance tumor immune monitoring (37,38). Meanwhile, knockdown of *ARHGAP11A* in normal and hypoxic environments showed that it can significantly reduce the expression of PDL1, HIF1A factor, VEGFA, and LDHA. From the past studies, we know that hypoxic tumors promote angiogenesis by overproducing angiogenic

growth factors (such as VEGF), to induce the formation of new blood vessels and promote tumor growth (39-41). The production of lactic acid during glycolysis contributes to the malignant progression to a great extent, such as supplementing and for glycolysis, reducing invasive pH, and triggering immune escape. LDHA converts pyruvate into lactic acid. The abnormal expression and activation of LDHA is closely related to a variety of cancers (42-44). The above results confirm that silencing of *ARHGAP11A* can affect the process of hypoxia and immune regulation. Finally, by interfering with the expression of *ARHGAP11A*, the apoptotic proteins BAX and Caspase-3 increased, whereas the anti-apoptotic proteins, G1/S phase conversion proteins CyclinD1 and CyclinE1, migration and invasion proteins MMP2 and MMP9, and proliferation proteins P-PI3K and P-AKT generally decreased (45-50). These findings suggest that *ARHGAP11A* is closely related to the occurrence and progression of tumors, elucidate the relationship between *ARHGAP11A* and the development of tumor cells in many aspects, and provide insights into the potential therapeutic mechanisms, which may be the basis for the individualized treatment of LUAD patients.

Conclusions

The expression of *ARHGAP11A* in LUAD is significantly correlated with immune invasion, hypoxia regulation, and prognostic development, suggesting that *ARHGAP11A* may be a good potential therapeutic target for complex TMEs.

Acknowledgments

A portion of the results of this study are based on TCGA (https://portal.gdc.cancer.gov/) and GEO (https://www.ncbi.nlm.nih.gov/geo/) databases.

Footnote

Reporting Checklist: The authors have completed the TRIPOD and MDAR reporting checklists. Available at https://tcr.amegroups.com/article/view/10.21037/tcr-24-224/rc

Data Sharing Statement: Available at https://tcr.amegroups.com/article/view/10.21037/tcr-24-224/dss

Peer Review File: Available at https://tcr.amegroups.com/article/view/10.21037/tcr-24-224/prf

Funding: This study received grants from the Key Projects of Scientific Research in Higher Educational Institutions in Anhui Province (2024AH051188), Bengbu Science and Technology Innovation Guidance Project (2024ZD0004), the Open Research Fund Project of Anhui Province Key Laboratory of Immunology in Chronic Diseases (No. KLICD-2023-Z4), National Innovation Program for College Students (No. 202210367076), Anhui Provincial Undergraduate Innovative Training Program (No. S202310367018), Bengbu City Science and Technology Innovation Guidance Projects (No. 2024ZD0004), Research Funds of Joint Research Center for Regional Diseases of IHM (No. 2024bydjk007), and Anhui Provincial Health Research Project (Nos. AHWJ2023A20289, AHWJ2023A10057).

Conflicts of Interest: All authors have completed the ICMJE uniform disclosure form (available at https://tcr.amegroups.com/article/view/10.21037/tcr-24-224/coif). The authors have no conflicts of interest to declare.

Ethical Statement: The authors are accountable for all aspects of the work in ensuring that questions related to the accuracy or integrity of any part of the work are appropriately investigated and resolved. The study was conducted in accordance with the Declaration of Helsinki (as revised in 2013).

References

1. Siegel RL, Miller KD, Jemal A. Cancer statistics, 2020. CA Cancer J Clin 2020;70:7-30.
2. Hirsch FR, Scagliotti GV, Mulshine JL, et al. Lung cancer: current therapies and new targeted treatments. Lancet 2017;389:299-311.
3. Valastyan S, Weinberg RA. Tumor metastasis: molecular insights and evolving paradigms. Cell 2011;147:275-92.
4. Corrales L, Matson V, Flood B, et al. Innate immune signaling and regulation in cancer immunotherapy. Cell

Res 2017;27:96-108.
5. Kim R, Emi M, Tanabe K. Cancer immunoediting from immune surveillance to immune escape. Immunology 2007;121:1-14.
6. Petrova V, Annicchiarico-Petruzzelli M, Melino G, et al. The hypoxic tumour microenvironment. Oncogenesis 2018;7:10.
7. Muz B, de la Puente P, Azab F, et al. The role of hypoxia in cancer progression, angiogenesis, metastasis, and resistance to therapy. Hypoxia (Auckl) 2015;3:83-92.
8. Brooks JM, Menezes AN, Ibrahim M, et al. Development and Validation of a Combined Hypoxia and Immune Prognostic Classifier for Head and Neck Cancer. Clin Cancer Res 2019;25:5315-28.
9. Noman MZ, Desantis G, Janji B, et al. PD-L1 is a novel direct target of HIF-1α, and its blockade under hypoxia enhanced MDSC-mediated T cell activation. J Exp Med 2014;211:781-90.
10. Deng B, Zhu JM, Wang Y, et al. Intratumor hypoxia promotes immune tolerance by inducing regulatory T cells via TGF-β1 in gastric cancer. PLoS One 2013;8:e63777.
11. Xu J, Zhou X, Wang J, et al. RhoGAPs attenuate cell proliferation by direct interaction with p53 tetramerization domain. Cell Rep 2013;3:1526-38.
12. Kreider-Letterman G, Carr NM, Garcia-Mata R. Fixing the GAP: The role of RhoGAPs in cancer. Eur J Cell Biol 2022;101:151209.
13. Dai B, Zhang X, Shang R, et al. Blockade of ARHGAP11A reverses malignant progress via inactivating Rac1B in hepatocellular carcinoma. Cell Commun Signal 2018;16:99.
14. Kagawa Y, Matsumoto S, Kamioka Y, et al. Cell cycle-dependent Rho GTPase activity dynamically regulates cancer cell motility and invasion in vivo. PLoS One 2013;8:e83629.
15. Chen S, Duan H, Xie Y, et al. Expression and prognostic analysis of Rho GTPase-activating protein 11A in lung adenocarcinoma. Ann Transl Med 2021;9:872.
16. Ligeti E, Welti S, Scheffzek K. Inhibition and termination of physiological responses by GTPase activating proteins. Physiol Rev 2012;92:237-72.
17. Tcherkezian J, Lamarche-Vane N. Current knowledge of the large RhoGAP family of proteins. Biol Cell 2007;99:67-86.
18. Etienne-Manneville S, Hall A. Rho GTPases in cell biology. Nature 2002;420:629-35.
19. Jaffe AB, Hall A. Rho GTPases: biochemistry and biology. Annu Rev Cell Dev Biol 2005;21:247-69.
20. Porter AP, Papaioannou A, Malliri A. Deregulation of Rho GTPases in cancer. Small GTPases 2016;7:123-38.
21. Popescu NC, Goodison S. Deleted in liver cancer-1 (DLC1): an emerging metastasis suppressor gene. Mol Diagn Ther 2014;18:293-302.
22. Xu K, Liu B, Ma Y. The tumor suppressive roles of ARHGAP25 in lung cancer cells. Onco Targets Ther 2019;12:6699-710.
23. Pan S, Deng Y, Fu J, et al. Decreased expression of ARHGAP15 promotes the development of colorectal cancer through PTEN/AKT/FOXO1 axis. Cell Death Dis 2018;9:673.
24. Hu Q, Lin X, Ding L, et al. ARHGAP42 promotes cell migration and invasion involving PI3K/Akt signaling pathway in nasopharyngeal carcinoma. Cancer Med 2018;7:3862-74.
25. Sun L, Zhang Y, Lou J. ARHGAP9 siRNA inhibits gastric cancer cell proliferation and EMT via inactivating Akt, p38 signaling and inhibiting MMP2 and MMP9. Int J Clin Exp Pathol 2017;10:11979-85.
26. Tian T, Chen ZH, Zheng Z, et al. Investigation of the role and mechanism of ARHGAP5-mediated colorectal cancer metastasis. Theranostics 2020;10:5998-6010.
27. Andrews LP, Yano H, Vignali DAA. Inhibitory receptors and ligands beyond PD-1, PD-L1 and CTLA-4: breakthroughs or backups. Nat Immunol 2019;20:1425-34.
28. Liu X, Kwon H, Li Z, et al. Is CD47 an innate immune checkpoint for tumor evasion? J Hematol Oncol 2017;10:12.
29. Akram A, Inman RD. Immunodominance: a pivotal principle in host response to viral infections. Clin Immunol 2012;143:99-115.
30. Petitprez F, de Reyniès A, Keung EZ, et al. B cells are associated with survival and immunotherapy response in sarcoma. Nature 2020;577:556-60.
31. Cabrita R, Lauss M, Sanna A, et al. Tertiary lymphoid structures improve immunotherapy and survival in melanoma. Nature 2020;577:561-5.
32. Rankin EB, Giaccia AJ. Hypoxic control of metastasis. Science 2016;352:175-80.
33. Soeda A, Park M, Lee D, et al. Hypoxia promotes expansion of the CD133-positive glioma stem cells through activation of HIF-1alpha. Oncogene 2009;28:3949-59.
34. Krishnamachary B, Penet MF, Nimmagadda S, et al. Hypoxia regulates CD44 and its variant isoforms through HIF-1α in triple negative breast cancer. PLoS One 2012;7:e44078.

35. Rooney MS, Shukla SA, Wu CJ, et al. Molecular and genetic properties of tumors associated with local immune cytolytic activity. Cell 2015;160:48-61.
36. Li B, Severson E, Pignon JC, et al. Comprehensive analyses of tumor immunity: implications for cancer immunotherapy. Genome Biol 2016;17:174.
37. Shaw RJ, Cantley LC. Ras, PI(3)K and mTOR signalling controls tumour cell growth. Nature 2006;441:424-30.
38. Xue G, Zippelius A, Wicki A, et al. Integrated Akt/PKB signaling in immunomodulation and its potential role in cancer immunotherapy. J Natl Cancer Inst 2015;107:djv171.
39. Cantelmo AR, Pircher A, Kalucka J, et al. Vessel pruning or healing: endothelial metabolism as a novel target? Expert Opin Ther Targets 2017;21:239-47.
40. Seeber A, Gunsilius E, Gastl G, et al. Anti-Angiogenics: Their Value in Colorectal Cancer Therapy. Oncol Res Treat 2018;41:188-93.
41. Ferrara N, Gerber HP, LeCouter J. The biology of VEGF and its receptors. Nat Med 2003;9:669-76.
42. Sheng SL, Liu JJ, Dai YH, et al. Knockdown of lactate dehydrogenase A suppresses tumor growth and metastasis of human hepatocellular carcinoma. FEBS J 2012;279:3898-910.
43. Le A, Cooper CR, Gouw AM, et al. Inhibition of lactate dehydrogenase A induces oxidative stress and inhibits tumor progression. Proc Natl Acad Sci U S A 2010;107:2037-42.
44. Fantin VR, St-Pierre J, Leder P. Attenuation of LDH-A expression uncovers a link between glycolysis, mitochondrial physiology, and tumor maintenance. Cancer Cell 2006;9:425-34.
45. Bukholm IK, Nesland JM. Protein expression of p53, p21 (WAF1/CIP1), bcl-2, Bax, cyclin D1 and pRb in human colon carcinomas. Virchows Arch 2000;436:224-8.
46. Linjawi A, Kontogiannea M, Halwani F, et al. Prognostic significance of p53, bcl-2, and Bax expression in early breast cancer. J Am Coll Surg 2004;198:83-90.
47. Shen Y, Sun Z, Shi P, et al. Anticancer effect of petroleum ether extract from Bidens pilosa L and its constituent's analysis by GC-MS. J Ethnopharmacol 2018;217:126-33.
48. Donnellan R, Chetty R. Cyclin E in human cancers. FASEB J 1999;13:773-80.
49. Kato JY, Sherr CJ. Inhibition of granulocyte differentiation by G1 cyclins D2 and D3 but not D1. Proc Natl Acad Sci U S A 1993;90:11513-7.
50. Nelson AR, Fingleton B, Rothenberg ML, et al. Matrix metalloproteinases: biologic activity and clinical implications. J Clin Oncol 2000;18:1135-49.

Cite this article as: Sun K, Wang L, Zhang X, Chen H, Wang Z, Zhang J, Wang X, Lian C. Specific effects of hypoxia-immune core gene *ARHGAP11A* on lung adenocarcinoma. Transl Cancer Res 2025;14(2):778-795. doi: 10.21037/tcr-24-224